# In Vivo and in Vitro Peripheral-Type Benzodiazepine Receptor Polymerization: Functional Significance in Drug Ligand and Cholesterol Binding †

**10 AUTHORS**, INCLUDING:

Franck Delavoie
French National Centre for Scientific Research
25 PUBLICATIONS 385 CITATIONS

SEE PROFILE

Jean Maccario
French Institute of Health and Medical Resea…
88 PUBLICATIONS 1,666 CITATIONS

SEE PROFILE

Jean-Jacques Lacapere
French National Centre for Scientific Research
99 PUBLICATIONS 3,482 CITATIONS

SEE PROFILE

Vassilios Papadopoulos
McGill University
325 PUBLICATIONS 12,783 CITATIONS

SEE PROFILE

# In Vivo and in Vitro Peripheral-Type Benzodiazepine Receptor Polymerization: Functional Significance in Drug Ligand and Cholesterol Binding[†]

Franck Delavoie,[‡,§] Hua Li,[‡,∥] Matthew Hardwick,[‡,⊥] Jean-Claude Robert,[§] Christoforos Giatzakis,[‡] Gabriel Péranzi,[§] Zhi-Xing Yao,[‡] Jean Maccario,[#] Jean-Jacques Lacapère,[§] and Vassilios Papadopoulos*,[‡]

*Division of Hormone Research, Departments of Cell Biology and of Pharmacology and Neurosciences, Georgetown University Medical Center, Washington, D.C. 20057, Unité INSERM U410, Faculté de Médecine Xavier Bichat, 16 Rue Henri Huchard, 75870 Paris Cedex 18, France, and Unité INSERM U472, 16 Avenue Paul Vaillant-Couturier, Batiment INSERM, 94807 Villejuif, France*

ABSTRACT: Peripheral-type benzodiazepine receptor (PBR) is an 18 kDa high-affinity drug ligand and cholesterol binding protein involved in various cell functions. Antisera for distinct PBR areas identified immunoreactive proteins of 18, 40, and 56 kDa and occasionally 72, 90, and 110 kDa in testicular Leydig and breast cancer cells. These sizes may correspond to PBR polymers and correlated to the levels of reactive oxygen species. Treatment of Leydig cells with human chorionic gonadotropin rapidly induced free radical, PBR polymer, and steroid formation. UV photoirradiation generates ROS species, which increased the size of intramembraneous particles of recombinant PBR reconstituted into proteoliposomes consistent with polymer formation, determined both by SDS−PAGE and by freeze−fracture electron microscopy. Spectroscopic analysis revealed the formation of dityrosines as the covalent cross-linker between PBR monomers. Moreover, photoirradiation increased PK 11195 drug ligand binding and reduced cholesterol binding capacity of proteoliposomes. Further addition of PK 11195 drug ligand to polymers increased the rate of cholesterol binding. These data indicate that reactive oxygen species induce in vivo and in vitro the formation of covalent PBR polymers. We propose that the PBR polymer might be the functional unit responsible for ligand-activated cholesterol binding and that PBR polymerization is a dynamic process modulating the function of this receptor in cholesterol transport and other cell-specific PBR-mediated functions.

The peripheral-type benzodiazepine receptor (PBR)[1] was initially described as a binding site for the benzodiazepine diazepam present in peripheral tissues (*1*). Although the tissue and cell distribution, subcellular localization, and pharmacological properties of this receptor have been extensively studied, only recently was it shown that the 18 kDa PBR protein is a high-affinity cholesterol and drug ligand binding protein (*2*, *3*). These properties might explain the reported contribution of PBR and effect of PBR drug ligands in numerous biological functions, including steroid biosynthesis, mitochondrial respiration, cell proliferation, and apoptosis (*4*−*6*).

The determining factors in identifying and purifying PBR in various tissues were (i) the successful detergent solubilization of the mitochondrial PBR retaining ligand binding (*7*−*9*), (ii) the development of diagnostic high-affinity drug ligands, such as the isoquinolinecarboxamide PK 11195 and the benzodiazepine Ro5-4864 (*10*, *11*), and (iii) the development of a photoaffinity probe specific for PBR, a nitrophenyl derivative of PK 11195 known as PK 14105 (*12*). This PK 14105 labeled a protein of 18 kDa (*12*), which was subsequently purified by several groups (*13*−*15*). The corresponding cDNA was cloned (*16*−*19*) and shown to code for a 169 amino acid protein of an 18.9 kDa molecular size in all species studied, with an approximately 80% homology between mammalian species (*5*). Despite these findings, there was no information about the structure of non-cross-linked and/or ligand-free PBR.

Additional lines of evidence suggested that the native PBR might be associated with other protein(s). Various groups reported that detergent-solubilized, photolabeled PBR eluted as a 170−210 kDa protein (*15*, *20*) and unlabeled PBR eluted

* Corresponding author. Phone: 202-687-8991. Fax: 202-687-7855. E-mail: papadopv@georgetown.edu.

‡ Georgetown University Medical Center.

§ Unité INSERM U410, Faculté de Médecine Xavier Bichat.

∥ Present address: Macrogenics Inc., Rockville, MD 20858.

⊥ Present address: Department of Urology, James Buchanan Brady Urological Institute Research Laboratories, The Johns Hopkins University Hospital, Baltimore, MD 21287.

# Unité INSERM U472.

[1] Abbreviations: CRAC, cholesterol recognition amino acid consensus; PBR, peripheral-type benzodiazepine receptor; recPBR, recombinant PBR; VDAC, voltage-dependent anion channel; 2,7-DCF, 2,7-dichlorofluorescein diacetate; DMEM, Dulbecco's modifed Eagle's medium; Ham's F-12, nutrient mixture F-12 Ham; DMPC, dimyristoylphosphatidylcholine; DMPE, dimyristoylphosphatidylethanolamine; FBS, fetal bovine serum; hCG, human chorionic gonadotropin; HRP, horseradish peroxidase; L/P, lipid to protein ratio; MDA-231, MDA-MB-231 cells; PK 11195, (2-chlorophenyl)-*N*-methyl-*N*-(1-methylpropyl)-3-isoquinolinecarboxamide; promegestone, 17,21-dimethyl-19-norpregn-4,9-diene-3,20-dione; P4, progesterone; RIA, radioimmunoassay; Ro5-4864, 4′-chlorodiazepam; ROS, reactive oxygen species; TTBS, Tween−Tris-buffered saline.

as a larger protein. In addition to the 18 kDa photolabeled protein, various groups identified another protein in the range of 30−35 kDa that could also be photolabeled with PK 14105 (*14*). This protein could be photolabeled using radiolabeled flunitrazepam (*21*), AHN 086 (*22, 23*), and diazepam (*24*) in tissues devoid of GABA$_A$/benzodiazepine receptor. In subsequent studies, McEnery et al. (*25*) presented evidence indicating that the PK 14105 photolabeled 18 kDa mito-chondrial PBR was associated with two proteins of 32 and 30 kDa, identified as the voltage-dependent anion channel (VDAC) and the adenine nucleotide carrier, respectively. Moreover, all three proteins migrated as a single peak of 70 kDa on a gel filtration column, consistent with the hypothesis that they are subunits of the same receptor complex (*25, 26*). It should be noted that in this experiment the 18 kDa protein was also isolated covalently labeled with PK 14105.

In an effort to visualize PBR in Leydig cell mitochondrial membranes, where we showed that PBR drug ligands increase mitochondrial cholesterol transport and steroid formation (*4, 27*), we used a combination of electron microscopy coupled to atomic force microscopy to study the distribution of gold immunolabeled PBR molecules (*28*). These studies suggested that the native receptor is a multi-meric complex composed on an average of 4−6 18 kDa PBR subunits and possibly one 34 kDa VDAC subunit important to confer benzodiazepine binding (*19*). Interestingly, addition of the gonadotropin hCG to Leydig cells induced a rapid increase in PBR ligand binding and redistribution of PBR molecules in large clusters (*29*).

To better understand PBR molecular structure and func-tion, one should approach its native ligand-free structure within the membranes. We recently successfully reconstituted isolated recombinant 18 kDa PBR protein in proteoliposomes and demonstrated that this protein alone could bind with high-affinity cholesterol and PK 11195 (*3*). In addition, we observed that this protein could also bind the Ro5-4864 with high affinity but with lower capacity, in agreement with a report by Joseph-Liauzun et al. (*30*). Thus, although the presence of VDAC may be important in conferring a higher capacity to the 18 kDa PBR protein to bind benzodiazepines and may participate in PBR function (*19, 25, 31*), it does not seem to play a determining role in its ability to bind drug ligands. In addition, other reports failed to observe a role for adenine nucleotide carrier in benzodiazepine ligand binding to the 18 kDa PBR protein (*30*).

Taken together, these studies indicate that the 18 kDa PBR protein in its native environment exists in various higher molecular mass complexes ranging from 30 to 200 kDa. As noted above, photolabeling of membrane extracts with various probes resulted in the identification of PBRs as 18 and 30−35 kDa proteins as well as a 70 kDa protein complex (*25*). Considering that the 18 kDa PBR protein has the ability to bind both benzodiazepine and isoquinolinecarboxamide drug ligands and that non-cross-linked and/or ligand-free PBR has not yet been isolated, questions are raised about the identity, formation, and function of the higher molecular mass PBR complexes in drug ligand and cholesterol binding.

We report herein that, in response to reactive oxygen species, the 18 kDa PBR protein forms polymers both in vitro and in vivo. These polymers are 18 kDa PBR monomers linked through dityrosine formation. Cholesterol binds better to PBR monomers than to polymers, whereas PBR drug ligands exhibit higher binding to PBR polymers. In addition, we suggest that the PBR polymer might be the functional unit responsible for ligand-activated cholesterol binding.

## EXPERIMENTAL PROCEDURES

*Cell Culture.* MA-10 mouse Leydig tumor cells were a gift from Dr. Mario Ascoli (University of Iowa). Cells were plated at low density for 24 h in DMEM/Ham's F-12 medium, 7.5% horse serum, and 5% FBS. After 24 h, the media were changed, and fresh media containing the indicated amounts of hCG for various time periods were added. Purified hCG (batch CR-125 of biological potency 11900 IU/mg) was a gift from National Institutes of Health (NIH). At the end of the incubation period, the cell media were saved for progesterone determination, and the cells were either dissolved in 0.1 N NaOH for protein determination or collected for immunoblot analyses. The MDA-231 cell line, obtained from the Lombardi Cancer Center, Georgetown University Medical Center, was grown in DMEM and 10% FBS as previously described (*32*). Cell incubations and manipulations were performed in the dark.

*Analysis of Oxidative Stress.* Levels of cellular oxidative stress were measured using the fluorescent probe 2,7-dichlorofluorescein diacetate (DCF; Molecular Probes, Inc.) as described (*33*). In brief, MA-10 or MDA-231 cells were cultured in 96-well plates. MA-10 cells were treated for the indicated time periods with or without hCG. At the end of the treatment cells were incubated in the presence of 50 $\mu$M DCF in PBS. Fluorescence was then quantified using the Victor$^2$ quantitative detection fluorometer (ECG-Wallac, Inc.). To determine the hCG-induced ROS levels, basal ROS values were subtracted from the hormone-induced values.

*Progesterone and Protein Measurements.* Progesterone levels were measured by means of RIA using [1,2,6,7-N-$^3$H]progesterone (specific activity 94.1 Ci/mmol) obtained from DuPont-New England Nuclear (Wilmington, DE) and antibodies from ICN Pharmaceuticals (Costa Mesa, CA). The data were analyzed using the MultiCalc software from EGG-Wallac, Inc. (Gaithersburg, MD). Protein levels were quanti-fied using the dye binding assay of Bradford (*34*) using bovine serum albumin as the standard.

*Antibodies Used and Immunoblot Analyses.* Rabbit anti-mouse PBR antibodies were raised against the following peptide sequences: VGLTLVPSLGGFMGAYFVR (ab-PBR-9−27; *2*), RGEGLRWYASLQK (ab-PBR-27−39; *35*), YIVWKELGGFTE (ab-PBR-65−76; *35*), LGGFTEDAM-VPLGLYTGQ (ab-PBR-71−88; *36*), and LNYYVWRDNS-GRRGGSR (ab-PBR-150−166). Ab-PBR-150−166 and antiserum against isolated recombinant mouse PBR protein (ab-recPBR) isolated as previously described (*2*) were raised in rabbits (Biosynthesis Inc., Lewsville, TX). From these antisera, only ab-PBR-9−27 was affinity purified on a column with immobilized peptide antigen (*2*). Anti-His tag antiserum was obtained from Novagen (Madison, WI). Cell and tissue protein samples were solubilized in sample buffer [25 mM Tris-HCl (pH 6.8), 1% SDS, 5% $\beta$-mercaptoethanol, 1 mM EDTA, 4% glycerol, and 0.01% bromophenol blue], boiled for 5 min, and loaded onto a 15% SDS−PAGE. Separated proteins were electrophoretically transferred to nitrocellulose membrane (Schleicher & Schuell Inc., Keene, NH). Membranes were incubated in blocking TTBS (20 mM

Tris-HCl, pH 7.5, 0.5 M NaCl, and 0.05% Tween-20) buffer containing 10% nonfat milk) at room temperature for 1 h, followed by incubation with a primary antibody against PBR (1:2000) for 2 h. Membranes were then washed with TTBS three times for 10 min each time. After 1 h incubation with the secondary antibody, goat anti-rabbit IgG conjugated with HRP (1:5000) (Transduction Laboratories, Lexington, KY), membranes were washed with TTBS three times for 10 min each time. Specific protein bands were detected by chemiluminescence using the Renaissance Kit (DuPont-New England Nuclear). In some occasions, the specificity of the bands recognized by the antibody was demonstrated using preabsorbed antibody prepared by incubating the antibody with the peptide used for the immunization.

*In Vitro Transcription and Translation of PBR.* Mouse PBR cDNA (*19*) was subcloned to the *Eco*RI−*Bam*HI site of pZeoSV2(−) plasmid (Invitrogen). In vitro transcription and translation of PBR were performed using the TNT quick coupled transcription/translation systems (Promega, Madison, WI) in the presence of [$^{35}$S]methionine (specific activity 1000 Ci/mmol) obtained from DuPont-New England Nuclear following the manufacturer's recommendations. The product of the reaction was incubated with MA-10 Leydig cell mitochondria isolated as previously described (*27*). Mitochondria were washed twice, and proteins were separated by SDS−PAGE on a 4−20% gradient acrylamide−bis-(acrylamide) gel at 125 V for 2 h and transferred to nitrocellulose membrane. The membrane was exposed to a multipurpose phosphor screen for 4 h and analyzed by phosphoimaging using the Cyclone storage phosphor system (Packard BioScience, Meridien, CT) or using X-film for overnight.

*Expression and Purification of recPBR.* The pET15PBR vector was used to transform the BL21(DE3) *Escherichia coli* strain (Novagen, Madison, WI) where the expression of recombinant mouse PBR protein was induced by 1 mM isopropyl 1-thio-β-D-galactopyranoside as previously described (*2, 37*). Cells were harvested in 150 mM NaCl and 50 mM phosphate, pH 7.4, washed in 300 mM NaCl and 50 mM phosphate, pH 7.4, and sonicated thoroughly. The pellet was collected at 20000*g* centrifugation and dissolved in binding buffer containing 0.5% SDS. The recPBR was purified by the His•Bind metal chelation resin (Novagen, Madison, WI) and stored in binding buffer with 1% SDS as previously described (*2*).

*[$^3$H]Promegestone Photolabeling.* Various concentrations of recPBR in PBS were incubated with [$^3$H]promegestone (specific activity, 94.1 Ci/mmol; NEN Life Science Products, Boston, MA) at a final concentration of 120 nM in the absence or presence of cholesterol (0.2 mM), progesterone (0.2 mM), pregnenolone (0.2 mM), testosterone (0.2 mM), 17β-estradiol (0.2 mM), or 22R-hydroxycholesterol (0.2 mM) (Sigma-Aldrich, St. Louis, MO) in a 100 μL final volume. After 1 h incubation at 4 °C, samples were photoirradiated for 30 min at a distance of <0.5 cm with a 366 nm lamp (UVP Inc., Gabriel, CA) as previously described (*2*). Sample loading buffer was applied to the samples, and they were submitted to SDS−PAGE. Proteins were transferred to nitrocellulose membranes, which were subsequently exposed to a tritium-sensitive screen and analyzed by the Cyclone storage phosphor system. Image analysis of the phospho-

rimages was performed using the OptiQuant software from Packard Biosciences Inc.

*Reconstitution of recPBR in Liposomes.* A stock solution of lipids (DMPC/DMPE, 9/1) was added to a SDS-containing buffer (50 mM NaPO$_4$ at pH 8, 150 mM NaCl) such that the final detergent to lipid ratio was equal to 2 (w/w). The solution was stirred for 30 min at room temperature before addition of the SDS-solubilized isolated recPBR protein at a concentration corresponding to the chosen lipid to protein ratio. The resulting micellar protein−lipid−detergent mixture was stirred for 15 min at room temperature before addition of Bio-Beads SM2, which remove SDS and induce vesicle formation (*3*). Bio-Beads were added in a two-step process: first, 1 g of Bio-Beads was added per 30 mg of SDS and mixed for 30 min; second, the same Bio-Beads amount was added and left for another 30 min. Bio-Beads were subsequently removed, and the solution was kept in the cold at 4 °C.

*Irradiation.* Fifty microliters of solubilized or reconstituted recPBR (0.2 mg/mL, i.e., 10$^{-5}$ M), in a microfuge tube ice-cooled in a water bath, was irradiated at 7.5−12 cm distance with a 254 nm UV lamp (Spectrolinker XL1000 UV cross-linker; Spectronics Corp., Rochester, NY) generating an energy of 1.2 mJ/cm$^2$. A 10 μL aliquot was taken at various incubation time periods, and the reaction was stopped by mixing with 5 μL of nonreducing sample buffer. Ten microliters (1.3 μg of recPBR) of the preparation was loaded onto SDS−PAGE (12.5% acrylamide). Separated proteins were visualized by silver staining (*38*). For the spectrofluorometric studies, a 2.5 mL cuvette containing 10$^{-8}$−10$^{-6}$ M reconstituted recPBR [L/P = 4 (w/w)] used in the fluorometer (Photon Technology Inc., Lawrenceville, NJ) was irradiated as described above; fluorescence spectra were recorded and compared to nonirradiated PBR. Aliquots (250 μL, 10$^{-7}$ M) were taken and centrifuged for 20 min at 60000*g* in a TL100 Beckman centrifuge, and pellets containing proteoliposomes were resuspended in 37.5 μL of nonreducing sample buffer. Samples (15 μL/0.12 μg of recPBR) were loaded onto SDS−PAGE (12.5% acrylamide). Separated proteins were visualized by silver staining. For freeze−fracture experiments, 0.35 mL of reconstituted recPBR [0.29 mg/mL; i.e., 1.5 × 10$^{-5}$ M L/P = 20 (w/w)], in a microfuge tube ice-cooled in a water bath, was irradiated under the same conditions as described above. A 6 μL aliquot was taken at various incubation times, and the reaction was stopped by mixing with 4 μL of nonreducing buffer. Samples (8 μL/1.3 μg of recPBR) were loaded onto SDS−PAGE (12.5% acrylamide). Separated proteins were visualized by silver staining.

*Spectroscopic Measurements.* Absorption spectra of tryptophan and tyrosine, added in a 2 mL cuvette containing PBS, were recorded with an UNICAM 300 spectrophotometer (Spectronic UNICAM) at room temperature before and after UV irradiation. Excitation and emission spectra were recorded with a PTI fluorometer (Photon Technology International) at room temperature before and after UV irradiation. Reconstituted recPBR (0.02 mg/mL, i.e., 10$^{-6}$ M), tryptophan, tyrosine, and dityrosine were added in a 2 mL cuvette containing PBS buffer at pH 7.8. The formation of dityrosines was performed at room temperature for 1 h as described by Malencik et al. (*39*), and the amount was determined by fluorescence spectroscopy determined in a 5 mL borate buffer

(pH 9.1) containing 5 mM tyrosine. Lactoperoxidase (100 $\mu$g) was added, and the reaction was initiated by addition of 14 $\mu$L of $H_2O_2$ (3%).

*Radioligand Binding Assays.* Reconstituted recPBR protein (0.5−2.0 $\mu$g/mL) in a 4/1 (w/w) lipid to protein ratio was used for PK 11195 and cholesterol ligand binding studies. Irradiated proteoliposomes were prepared as described above. [$^3$H]PK 11195 (specific activity 83.5 Ci/mmol; NEN Life Science Products) and [1,2-$^3$H]cholesterol (specific activity 43.8 Ci/mmol; NEN Life Science Products) binding studies were performed as previously described (*3*, *27*). Bound [$^3$H]-PK 11195 and [$^3$H]cholesterol were quantified by liquid scintillation spectrometry. Dissociation constants ($K_d$), the number of binding sites ($B_{max}$), and Hill coefficients ($n_H$) for PK 11195 and cholesterol were determined by Curve-Fit (Prism version 3.0; GraphPad Software Inc., San Diego, CA).

*Electron Microscopy.* Samples (300 $\mu$L) of UV-irradiated proteoliposomes were centrifuged and resuspended in 50 $\mu$L of 10 mM MOPS−KOH (pH 7.0). Samples were freeze-fractured and coated initially with platinum under a 45° angle and then with carbon at a 90° angle in a Balzers apparatus (Balzers, Lichtenstein) with a total deposit calibrated at ca. 20 nm. Biophysical examination of samples was made in a JEOL 1200 EX electron microscope operated at 80 kV accelerated voltage (magnification: 120000×). Measurements of the intravesicular particles were made as previously described (*3*). In brief, measurements of coating shadows (platinum/carbon) over vesicular particles were made directly from the electron microscopic negatives. A Biocom 200 photometric image analysis system and Imagenia software (Imagenia et Instrumentation Biotechnologique, Les Ulis, France) were strictly applied to minimize the possibility of measuring error. The computer program provided isodensitometric contours of all shadows, and in addition, it applied morphometric parameters to the same contours. The population of diameters was a mixture of log normal populations. The parameters of the mixture (i.e., proportions, mean and standard deviation of each component) were estimated by maximum likelihood. The concordance of empirical and estimated distributions was assessed by examination of the PP plot. The best concordance is generally obtained when the plot follows the first diagonal.

*Statistics.* Statistical analysis was performed by one-way ANOVA and unpaired Student's *t* test using the INSTAT 3.00 package from GraphPad.

## RESULTS

*Detection of PBR Polymers in Vivo and Correlation with ROS Levels.* During the past decade, we developed a number of antisera against various regions of the PBR protein (*2*, *35*, *36*) as well as antisera against the entire recPBR protein (present paper). Although these antisera recognized with various degrees of sensitivity the 18 kDa PBR protein, we consistently observed that they recognized additional proteins of 36−40 and 52−56 kDa, and in some cases 72, 90, and 110 kDa with various intensities (data not shown). For example, in MA-10 Leydig cells, ab-PBR-9−27 recognized mostly the 18 kDa PBR protein whereas ab-PBR-71−88 recognized also proteins of 40 and 54 kDa molecular mass (Figure 1A,C). In MDA-231 breast cancer cells, ab-PBR-9−27 and ab-PBR-71−88 recognized predominantly a 40

kDa protein although faint bands at 18 and 56 kDa molecular mass levels were seen (Figure 1A,C). The specificity of the immunoreactivities was demonstrated by preabsorbing ab-PBR-9−27 with the peptide used to generate this antiserum (Figure 1B). Interestingly, recPBR protein, which has a slightly higher molecular size than the native protein because of the presence of the His tag, was also found to generate an immunoreactive band around 40 kDa, which could not be seen with the peptide preabsorbed antiserum (Figure 1A,B). The presence of these complexes was more pronounced when cells or cell lysates were exposed to daylight. Treatment of the samples with increasing concentrations of SDS, ethanol, heat, chaotropic agents such as urea and guanidinium isothiocyanate, and PBR drug ligands failed to break these (40 and 56 kDa) proteins to smaller molecular mass proteins, suggesting that they involve covalent cross-links (data not shown). Because of the abundance of the higher molecular size PBR immunoreactive proteins in breast cancer cells and Alzheimer's disease hippocampus specimens (data not shown) that are known to contain high levels of ROS, we measured ROS in the cells examined to assess whether there were a correlation between ROS levels and the presence of high molecular mass PBR immunoreactive proteins. Indeed, MDA-231 cells contained higher ROS levels compared to MA-10 Leydig cells (Figure 1D).

*Polymer Formation by in Vitro Transcribed and Translated PBR.* To examine the ability of PBR to form polymers, mouse PBR cDNA was in vitro transcribed and translated and the protein incorporated into MA-10 Leydig cell mitochondria. [$^{35}$S]Methionine labeling of the protein allowed following the incorporation of PBR into mitochondria. Figure 2A shows that a major 18 kDa radiolabeled protein was formed and incorporated into mitochondria. In addition to the 18 kDa protein, radiolabeled products of 36, 54, and 72 kDa were formed and incorporated into mitochondria. An incomplete 10 kDa PBR protein fragment was also formed, leading to the formation of intermediate 28, 46, and 64 kDa radiolabeled proteins.

*Dimer and Polymer Formation by Recombinant PBR in Solution.* We recently reported the expression and isolation from bacteria of recombinant mouse PBR with a His tag at the N-terminus (*2*, *37*). As noted above, the addition of the His tag results in the expression of a 20 kDa, instead of 18 kDa, PBR protein (*2*). During these studies we observed that recombinant PBR appears as both a 20 and a 40 kDa protein identified with antibodies raised against PBR (ab-PBR-9−27) and His tag (Figure 2B). These data suggest that these proteins correspond to PBR monomers and dimers.

To study the interaction of cholesterol with the isolated recombinant PBR, we used the progestin, [$^3$H]promegestone (*2*). [$^3$H]Promegestone was cross-linked by photoirradiation to the recombinant PBR (Figure 2C−E). [$^3$H]Promegestone cross-linking to the recombinant PBR was displaced by cholesterol (*2*; Figure 2C). However, in the presence of other steroids (progesterone, pregnenolone, 17$\beta$-estradiol, testosterone), we observed the appearance of 40, 60, and 80 kDa radiolabeled proteins in addition to the 20 kDa PBR protein (Figure 2C). The formation of these PBR polymers, in the presence of progesterone, was increased with a longer exposure to UV light, where additional PBR polymers of 100 and 120 kDa were seen after 30 min exposure. (Figure 2D). The formation of these polymers was also dependent
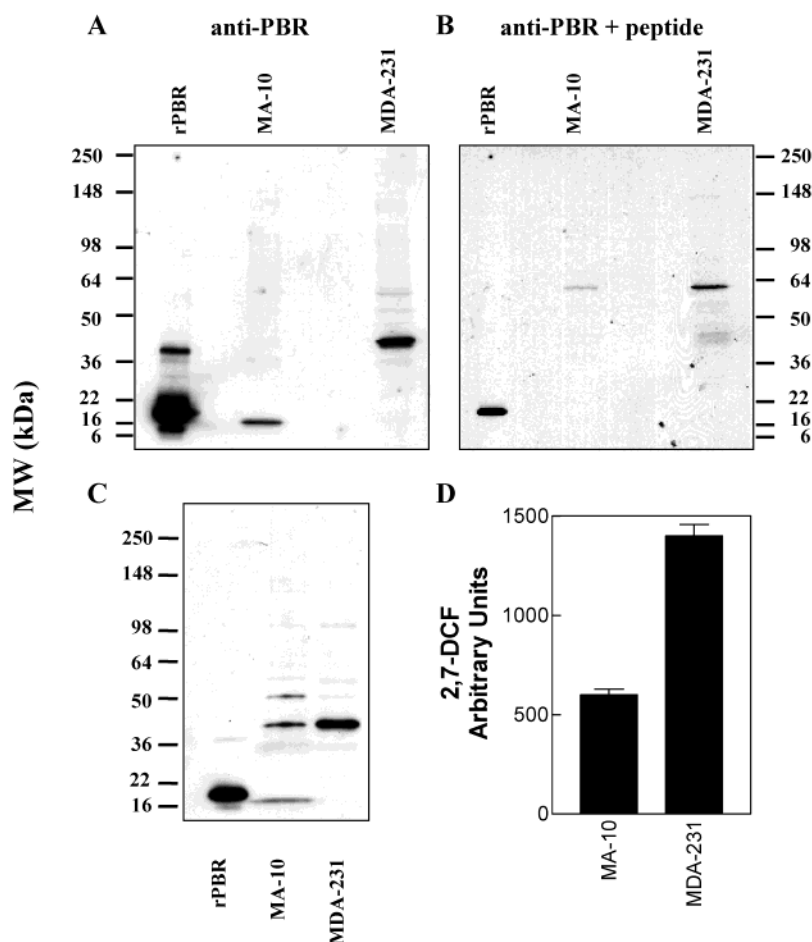
FIGURE 1:  Detection of PBR polymers in vivo and correlation with ROS levels. (A) Immunoblot analysis of MA-10 Leydig and MDA-231 breast cancer cell extracts using ab-PBR-9−27 anti-PBR antiserum. (B) Specificity of the immunoreactivities seen in (A) examined by preabsorbing ab-PBR-9−27 with the peptide used to generate the antiserum. (C) Immunoblot analysis of MA-10 Leydig and MDA-231 breast cancer cell extracts using ab-PBR-71−88 anti-PBR antiserum. (D) ROS levels measured in MA-10 Leydig and MDA-231 breast cancer cells as described under Experimental Procedures.

on the amount of progesterone present during the photoirradiation process (Figure 2E). These data suggest that cholesterol, which was otherwise shown to bind with high affinity to PBR (2, 3), prevents covalent PBR cross-linking. In contrast, other steroids and UV light appear to favor this process (Figure 2C).

*Dimer and Polymer Formation by recPBR Reconstituted in Proteoliposomes.* UV-induced PBR cross-linking was also revealed by silver staining of solubilized PBR preparations (Figure 3, left). We recently reported that solubilized PBR maintained its ability to bind cholesterol, although with low affinity, but failed to bind PBR drug ligands (2). This problem was overcome by reconstitution of the recombinant PBR into proteoliposomes [at a lipid to protein ratio, L/P, of 4 (w/w)] (3). Reconstituted PBR bound with nanomolar affinities both cholesterol and PK 11195 (3). Here, we examined the effect of UV photoirradiation on reconstituted PBR. Figure 3, right, shows that UV exposure induces PBR polymer formation in a time-dependent manner.

*Hormonal Induction of PBR Polymers in MA-10 Leydig Cells.* The data presented above suggested that UV exposure was the cause of PBR polymer formation. Preliminary experiments indicated that the effect of UV exposure was mostly independent of the wavelength used. UV is a well-known inductor of free radical formation. Isolated protein

oxidation in response to UV and ROS is well documented (40). However, proteins in living cells are exposed to endogenously generated ROS rather than UV light. Considering the data presented in Figure 1, we looked for a physiological mechanism inducing ROS production in MA-10 Leydig cells. Taking into account our previous data on the rapid hCG-induced formation of PBR clusters (29) and reports showing that under physiological conditions LH increases lipid peroxidation in the testis (41) and that in the corpus luteum LH increases progesterone secretion and ROS production (42), we measured ROS and progesterone levels in response to hCG. Indeed, hCG induced both ROS and progesterone formation in a concentration-dependent manner (Figure 4A). Interestingly, the hCG generation of ROS is a very rapid phenomenon (Figure 4B) that occurs much faster than the synthesis of progesterone, because it can be seen within 1 min upon addition of the hormone. Simultaneously, the addition of hCG to MA-10 Leydig cells rapidly induces the formation of PBR polymers within 1 min (Figure 4C), in agreement with our previous data (29).

*Spectrophotometric Characterization of PBR Polymers in Proteoliposomes.* To characterize the type of covalent bond involved in PBR polymer formation, we performed a series of spectrophotometric studies. Figure 5A shows a silver-stained gel of photoirradiated reconstituted PBR (0.1 μM)
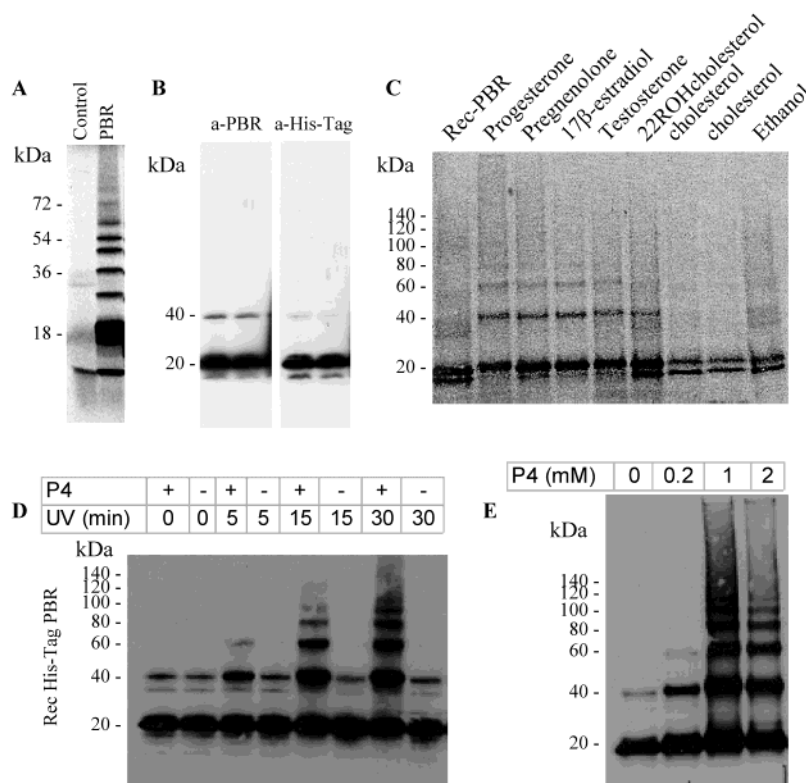
FIGURE 2: Dimer and polymer formation by in vitro transcribed and translated PBR and by recombinant PBR in solution. (A) Mouse PBR cDNA was in vitro transcribed and translated and the radiolabeled protein product(s) incorporated into MA-10 Leydig cell mitochondria. Proteins were separated by SDS−PAGE, and radiolabeled proteins were visualized by phosphorimaging. (B) Immunoblot analysis of recPBR using ab-PBR-9−27 and anti-His tag antisera. (C) Isolated recombinant PBR (5 $\mu$M) incubated with [$^3$H]promegestone in the presence or absence of the indicated steroids at 0.2 mM concentration. Samples were exposed to UV light, and at the end of the incubation the samples were separated by SDS−PAGE. (D) Isolated recombinant PBR (5 $\mu$M) was incubated with [$^3$H]promegestone in the presence or absence of the 1 mM progesterone (P4). Samples were exposed to UV light for the indicated time periods, and at the end of the incubation the samples were separated by SDS−PAGE. (E) Isolated recombinant PBR (5 $\mu$M) incubated with [$^3$H]promegestone in the presence or absence of the indicated concentrations of progesterone (P4). Samples were exposed to UV light for 30 min, and at the end samples were separated by SDS−PAGE. In (B), (C), and (D) photoincorporation of [$^3$H]promegestone to recombinant PBR was detected by phosphorimaging.

at L/P 4. Mouse PBR contains 12 tryptophan and 10 tyrosine residues that might be responsible for intrinsic fluorescence of the receptor. Figure 5B shows that PBR intrinsic fluorescence decreased upon UV exposure at 290 nm (excitation), suggesting that some tryptophans might be involved in polymer formation. As a control we examined the effect of UV irradiation on a solution of tryptophan. Panels C and D of Figure 5 show a UV-induced tryptophan fluorescence decrease in the emission spectra when excited at 290 nm (Figure 5C) and a fluorescence increase when excited at 320 nm with a maximum emission wavelength at 440 nm (Figure 5D), which might indicate the formation of ditryptophans (*43*). To examine whether such phenomenon occurs in the UV-exposed reconstituted PBR, we measured the fluorescence spectra of PBR excited at 320 nm. Figure 5E shows that reconstituted PBR exposed to UV shows a maximum emission wavelength at 380 nm when excited at 320 nm, indicating that ditryptophans are not involved in PBR polymer formation.

Considering that ROS have been shown to lead to covalently stable bond formation via dityrosine formation (*40*, *44*, *45*), we further examined if such reaction might occur in our system. Figure 5F shows that UV irradiation of a tyrosine solution induces an increase in fluorescence with a maximum emission at 390 nm when excited at 320 or at 290 nm, in agreement with dityrosine formation (*39*).
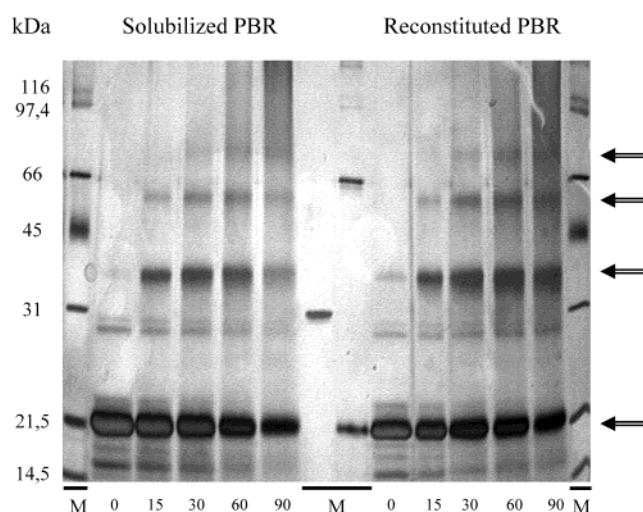


FIGURE 3: Dimer and polymer formation by recPBR reconstituted in proteoliposomes. Silver-stained SDS−PAGE of UV-irradiated PBR (10 $\mu$M) either solubilized or reconstituted in liposomes (DMPC/DMPE, 9:1) at a lipid/protein ratio of 4 (w/w) at 4 °C. Irradiation times (minutes) are shown at the bottom of the lanes. Molecular mass standards (M) are shown in the first, middle, and last lanes. The middle lanes show carbonic anhydrase (31 kDa), serum albumin (66 kDa), and trypsin inhibitor (21.5 kDa) molecular mass standards in the range of PBR monomers, dimers, and trimers. Arrows on the right indicate the molecular sizes corresponding to PBR monomers, dimers, trimers, and tetramers.
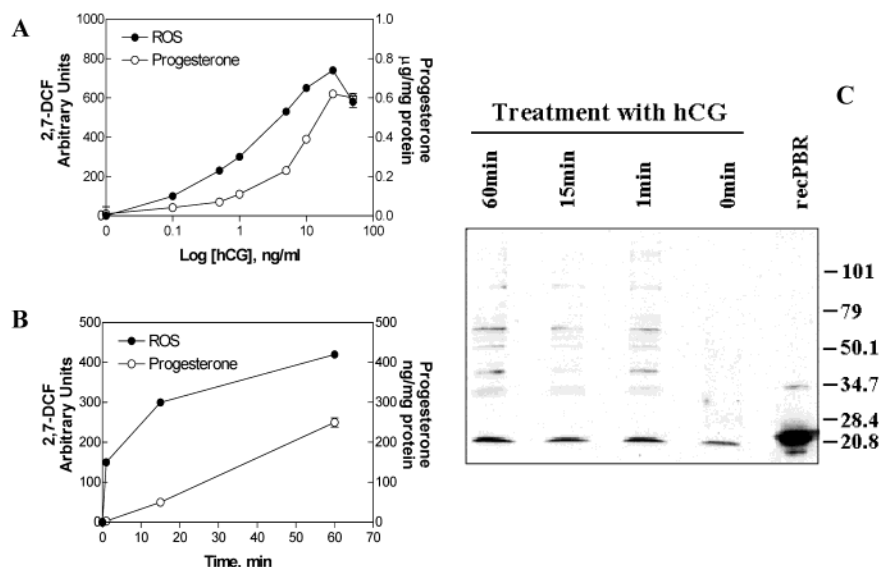
FIGURE 4: Hormonal induction of PBR polymers, ROS formation, and progesterone synthesis in MA-10 Leydig cells. (A) MA-10 Leydig cells were treated with the indicated concentration of hCG for 30 min. (B) MA-10 Leydig cells were exposed to 50 ng/mL hCG for the indicated time periods. For both (A) and (B), at the end of the incubation ROS and progesterone were determined as described under Experimental Procedures. Results shown are means ± SD from four independent experiments ($n = 12$). (C) Immunoblot analysis of MA-10 Leydig treated for the indicated time periods in the dark with 50 ng/mL hCG using the ab-PBR-9−27 antiserum.

Because the 390 nm maximal emission measured with dityrosine solution is close to the 380 nm observed for UV-irradiated PBR, it is proposed that ROS-induced PBR cross-linking involves dityrosine formation. The amplitude of the dityrosine fluorescence observed with PBR suggests that only one or two tyrosines per monomer are cross-linked.

*Morphological Characterization of PBR Polymers in Proteoliposomes.* Figure 6A shows a silver-stained gel of reconstituted PBR at L/P 20 (w/w), photoirradiated for 15, 30, 60, and 90 min, respectively. A 90 min irradiation induced the formation of dimers and small amounts of trimers shown by arrows. Freeze−fracture experiments (Figure 6B−I) were performed to characterize the transmembranous domain of nonirradiated (Figure 6B) and 90 min irradiated (Figure 6C) PBR reincorporated in the bilayer. Figure 6D−I shows different types of particles observed in freeze-fractured proteoliposomes. Panels D and E of Figure 6 correspond to typical monomers. Figure 6F−I corresponds to the dimer, trimer, possible tetramer, and higher polymers of PBR, respectively. Figure 7 shows the distribution of the diameter of intravesicular particles in nonirradiated (Figure 7A) and 90 min irradiated (Figure 7B) PBR proteoliposomes. Histograms showing nonirradiated samples (Figure 7A) revealed two populations of particles. The median width of the first group of particles, representing 52% of the population, was of 8.0 ± 1.6 nm apparent diameter. The median width of the second group of particles, representing 48% of the population, was 12.0 ± 2.5 nm. Histograms of data obtained from irradiated samples (Figure 7B) can be analyzed with three populations of particles. The median width of the first group of particles, representing 53% of the population, was 8.0 ± 1.7 nm. The median width of the second group of particles, representing 45% of the population, was 13.0 ± 2.4 nm. The median width of the third group of particles, representing 2% of the population, was 22.0 ± 1.1 nm. The concordance of empirical and estimated distributions of control and irradiated data was assessed by examination of the percentile percentile (PP) plot (panels C and D of Figure

7, respectively). The data presented in Figure 7 show that irradiated and nonirradiated samples contain both PBR monomer and dimer in almost equal proportions. However, under the conditions used (L/P 20), only the irradiated samples contain higher PBR polymer in small proportion. Because of the limited size of this polymeric PBR population, in agreement with the SDS−PAGE shown in Figure 6A, the characterization of trimer and tetramer was difficult to achieve, and for this purpose the respective positions of these PBR polymers are indicated by arrows on Figure 7B. It should be noted that the percentage of each population observed in the freeze−fracture experiments does not directly correspond to the band intensity for PBR monomer and polymers seen on SDS−PAGE (Figure 6A). The diameters measured described mostly monomers and small-size polymers and to a much lesser extent higher molecular mass polymers. A closer look at the histograms shown in Figure 7 indicates the presence of four picks (arrows in Figure 7B) corresponding to monomers, dimers, trimers, and tetramers. Because the percentages of trimer and to a lesser extent tetramer population are very low compared to monomer and dimer PBR, the mathematical analysis used was not able to detect them. This was not due to the number of samples used, because histogram profiles were the same counting either 1000 or 1200 particles. Since these measurements were made directly from the platinum/carbon layers, it was necessary to establish the corrected value of the intravesicular particles alone. The latter value was calculated as the directly measured value minus the thickness of the deposited replica (*3*, *46*, *47*). Consequently, the corrected average sizes for the three populations were derived as 3.5, 7.0, and 14 nm, respectively, suggesting the presence of monomers, dimers, and tetramers.

*Drug Ligand and Cholesterol Binding Properties of PBR Polymers in Proteoliposomes.* Reconstituted PBR (L/P 4) binds with high affinity both PK 11195 (1.5 nM; Figure 8B) and cholesterol (6.0 nM; Figure 8D), in agreement with our previous studies (*3*). UV photoirradiation of the reconstituted
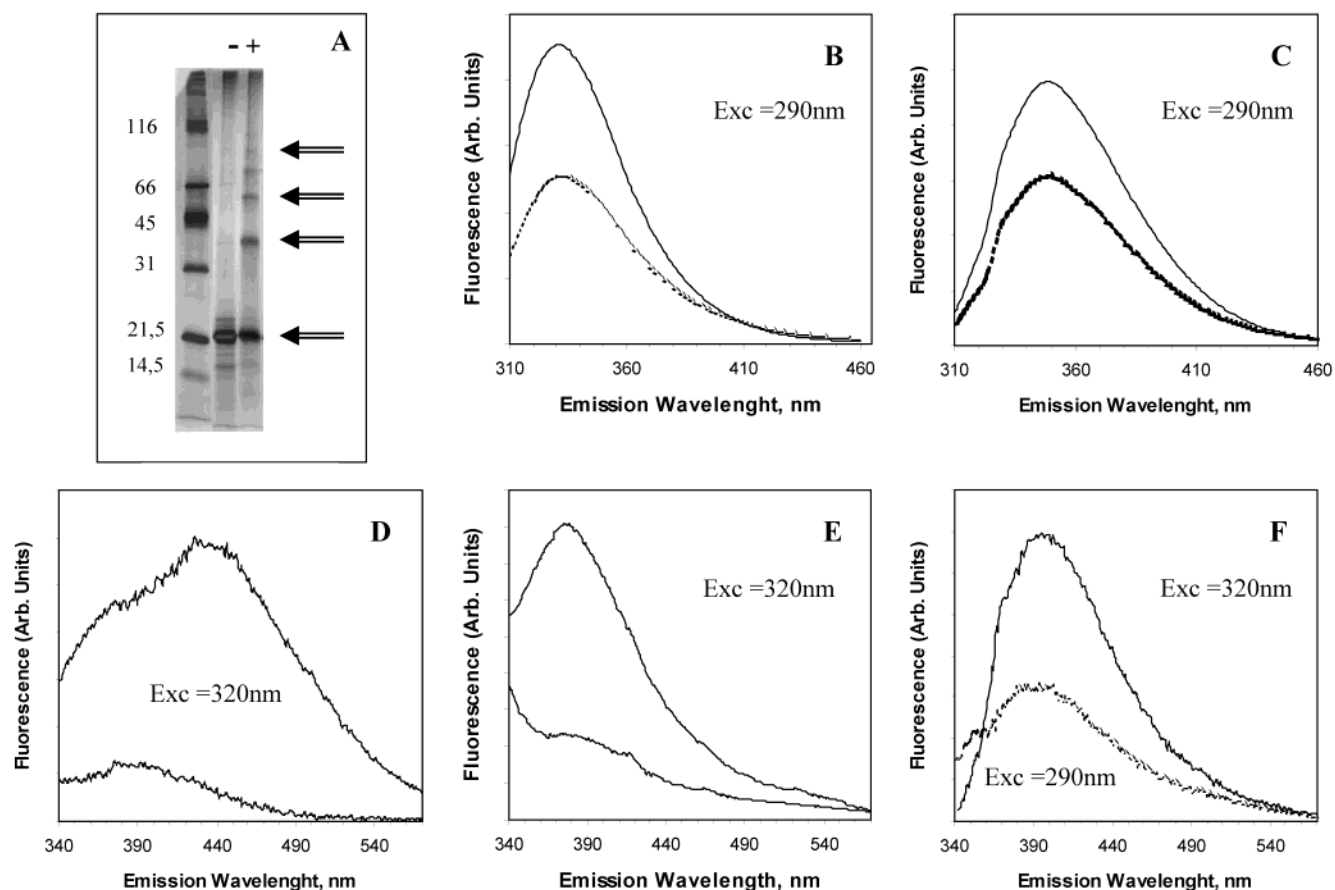
FIGURE 5: Spectrophotometric characterization of PBR polymers in proteoliposomes. (A) Silver-stained SDS−PAGE of PBR reconstituted in liposomes (DMPC/DMPE, 9:1) at a lipid/protein ratio of 4 (w/w) at 4 °C and UV irradiated for 30 min. recPBR (100 nM) was used for photoirradiation. Molecular mass standards are shown in the first lane. Arrows on the right show molecular sizes corresponding to PBR monomers, dimers, trimers, and tetramers. (B) Emission fluorescence spectra of PBR (1 $\mu$M) measured at 290 nm excitation wavelength. Upper line: spectrum before 30 min UV light irradiation in PBS. Bottom line: spectrum after irradiation. (C) Tryptophan (5 $\mu$M) fluorescence emission spectra measured at 290 nm excitation wavelength. Upper line: spectrum before 30 min UV light irradiation in PBS. Bottom line: spectrum after irradiation. (D) Tryptophan (5 $\mu$M) fluorescence emission spectra measured at 320 nm excitation wavelength. Bottom line: spectrum before 30 min UV light irradiation in PBS. Upper line: spectrum after irradiation. (E) Emission fluorescence spectra of PBR (1 $\mu$M) before (bottom line) and after (upper line) UV light irradiation measured at 320 nm excitation wavelength. (F) Tyrosine (10 $\mu$M) fluorescence emission spectra determined at either 320 nm (upper line) or 290 nm (bottom line) excitation wavelengths after 30 min UV light irradiation.

PBR induced a time-dependent increase in PK 11195 ligand binding that reached its maximum at 45 min exposure time and dropped thereafter (Figure 8A). Saturation isotherm analysis of the samples submitted to 45 min irradiation time indicated that the UV-induced increase in PBR ligand binding was due to a 5-fold increase in the PK 11195 ligand binding capacity, with a minor 2-fold decrease in affinity (Figure 8B). In contrast, photoirradiation induced a time-dependent decrease in cholesterol binding (Figure 8C). Saturation isotherm analysis at 45 min irradiation time indicated that the UV-induced decrease in cholesterol binding was due to a 2.7-fold reduction in cholesterol binding capacity, with a significant 6.7-fold increase in affinity (Figure 8D). These data suggest that cholesterol binds to both PBR monomers and polymers and that polymer formation results in increased PBR drug ligand binding associated with a decreased cholesterol binding. On the basis of our previous data on the effect of progesterone on formation of promegestone-radiolabeled PBR polymers upon photoirradiation (Figure 2C), we examined the effect of progesterone on the ability of PBR polymers to bind PK 11195. Progesterone (1 $\mu$M) abolished the ability of PBR polymers to bind PK 11195 in time-dependent manner (Figure 8A, open symbols).

*Ligand-Induced Cholesterol Binding by PBR Polymers in Proteolipososmes.* One of the most extensively studied and established functions of PBR is its role in mediating the transport of cholesterol into the mitochondria of steroidogenic cells (*4*, *6*). This function, which probably consists of a number of steps including cholesterol binding, uptake, and release, has been shown to be activated by PK 11195 in all steroidogenic cells tested. To investigate the first step of this function of PBR in the in vitro reconstituted PBR system, we examined the effect of PK 11195 on the ability of reconstituted PBR to bind cholesterol before and after UV irradiation, i.e., monomeric versus polymeric PBR. Figure 9 shows that PBR polymer formation resulted in a dramatic and rapid ($t_{1/2} = 0.5$ min) PK 11195 (100 nM) dependent increase in cholesterol binding. This is a transient effect that reaches a maximum at 3 min and decreases thereafter. Conversely, monomeric (i.e., nonirradiated) PBR binds slowly ($t_{1/2} = 6$ min) cholesterol in response to PK 11195 and in a monoexponential manner (Figure 9, squares). Addition of 1 $\mu$M progesterone in the reaction mixture abolished cholesterol binding by the PBR polymers (Figure 9, open symbols).
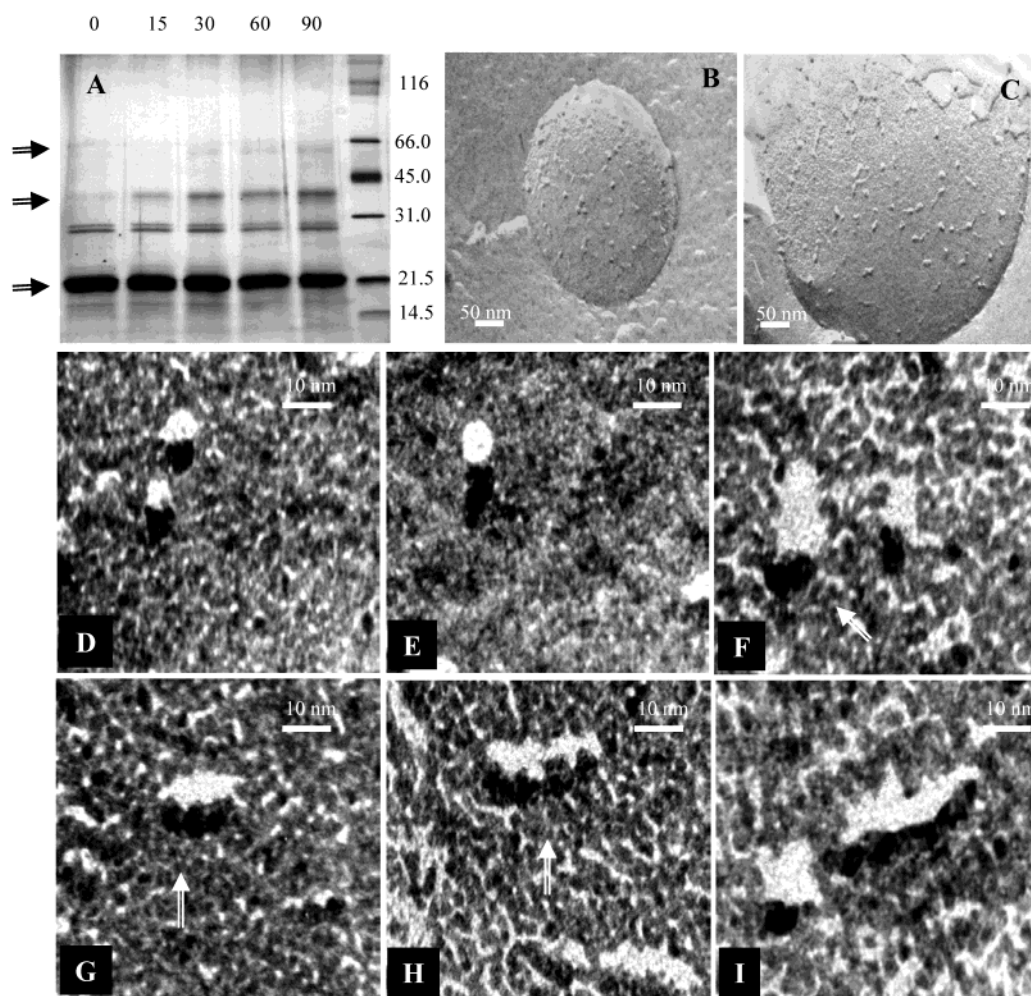
FIGURE 6: Morphological characterization of PBR polymers in proteoliposomes. Silver-stained SDS−PAGE (A) of UV-irradiated PBR reconstituted in liposomes (DMPC/DMPE, 9:1) at a lipid/protein ratio of 20 (w/w) at 4 °C. The different irradiation times used (minutes) are shown on the top of the gel. Molecular mass standards (kDa) are shown in the last lane. Arrows on the left indicate molecular sizes of the PBR monomers, dimers, and trimers. Freeze-fractured control proteoliposomes are shown in (B) and freeze-fractured 90 min UV-photoirradiated proteoliposomes are shown in (C). Panels D−I show representative types of objects observed in freeze-fractured proteoliposomes: (D, E) typical monomers; (F) dimer (arrow); (G) trimer (arrow); (H) possible tetramer (arrow); (I) complex structure of oligomer. Please note the shadowing direction from bottom to top; white shadow convention.

## DISCUSSION

The synthesis and availability of a number of high-affinity drug ligands for PBR allowed the investigation of the function of this primarily mitochondrial membrane protein in various biological systems. To date, PBR has been described as one of the key proteins in several cell functions including the transport of cholesterol into the mitochondria in steroidogenic tissues (4), mitochondrial respiration (48), and cell proliferation in various tumor cell lines (39, 49, 50). It has also been shown to be a marker of cell growth and tumor formation (32, 49, 50) and a component of the permeability transition pore of the mitochondrial membrane involved in apoptosis (51−54). Moreover, PBR drug ligands are under evaluation for their ability to regulate neurosteroid synthesis and brain function, to detect tumor cells in vivo, and to induce or protect against apoptosis with major therapeutic consequences in cancer therapy (55).

It might not be just a coincidence that excessive ROS production occurs in mitochondria, where PBR is mainly found. Indeed, the data presented herein strongly suggest that PBR is a target for ROS. PBR at first reacts by forming covalent polymers, mediators of physiological functions. Under physiological conditions this could be a cycling process, where newly formed PBR monomers take the place of the polymerized PBR destined to be degraded. However, excessive levels of ROS or continuous exposure to ROS could lead to the continuous covalent polymerization of all of the newly formed PBR, thus leading to the exclusive presence of higher polymers, which could be detrimental to mitochondrial function and ultimately cell viability or, alternatively, to a new pathological state, i.e., in cancer cells.

The serendipitous discovery of PBR polymers was based on the observation that various PBR antisera recognized with various degrees of sensitivity the 18 kDa PBR protein in addition to proteins of 36−40, 52−56, 72, and 110 kDa (see Figures 1 and 4). Despite the observation that these proteins had molecular size multiples of the 18 kDa protein, for a long time our focus was centered either exclusively around the 18 kDa protein or on the presence of other proteins reported to be associated with the 18 kDa PBR protein. Interestingly, there were numerous reports on the presence of a 30−36 kDa protein shown to bind exclusive PBR drug
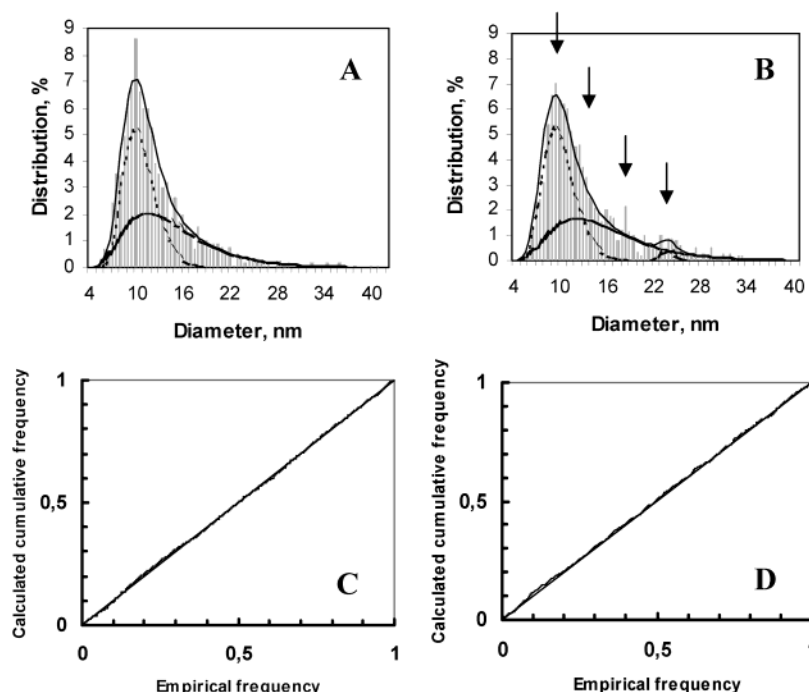
FIGURE 7: Morphometrical analysis of reconstituted recombinant PBR. Distribution of diameters of intravesicular particles from freeze-fractured control (A) and samples irradiated for 90 min (B). The calculated distributions are shown as continuous lines. The upper curves are the sum of the two (control) or the three (irradiated) populations. The other curves in each figure are representative of each individual subpopulation. Percentile percentile (PP) plot of the empirical and calculated models shows the concordance of the empirical (dotted line) and calculated (solid line) distribution of control (C) and irradiated (D) data.

ligands that were dismissed as being due to the association of this protein with PBR (*14, 21−24*). A careful examination of the PBR literature also unveiled that the first paper reporting the isolation of the photolabeled 18 kDa PBR protein also identified proteins of 32−36 and 50−54 kDa molecular size that were specifically radiolabeled by PK 14105, in addition to the 18 kDa PBR protein, in CHO hamster ovary mitochondrial cell extracts (*14*).

The observation that the 18 kDa PBR protein was organized in clusters of 2−7 molecules on the Leydig cell mitochondrial membrane suggested for the first time the presence of PBR polymers (*28*). The hormone-induced appearance of bigger PBR clusters concomitant with the appearance of a higher PBR ligand binding site and initiation of cholesterol transfer into mitochondria and steroidogenesis indicated that the formation of these clusters might be part of a functional process (*29*).

Considering the abundance of PBR in the mitochondrial membrane and its close association with numerous other proteins, it has been impossible to purify the native PBR protein. Thus, to understand the structure and function of this protein, we focused on isolating and characterizing a functional recombinant protein. The isolation of such a protein allowed us to first demonstrate that it had the ability to bind cholesterol in the carboxy terminus of the molecule (*2*). However, the absence of the drug ligand binding site in the solubilized PBR protein prompted us to proceed in reconstituting the protein into proteoliposomes. It was not until we succeeded in reconstituting a functional PBR in proteoliposomes (*3*) that the structure and function of PBR could be studied in a detailed manner.

During our search of PBR function in health and disease we examined PBR protein expression in various normal and pathological cells and tissues, including Leydig cells (*27*)

and breast cancer cells of various aggressive potential (*32*). The data obtained indicated the presence of PBR immunoreactive proteins of 18 kDa polymers (dimers and trimers) in breast cancer cells. Interestingly, these samples contained higher levels of free radicals compared to control samples. The presence of increased ROS in human breast cancer cells has been previously described and proposed as one of the determining parameters of breast carcinogenesis and metastasis (*56, 57*).

Most of our work during the past decade has been focused on the role of PBR in cholesterol transport and steroid production in testicular Leydig cells in response to the gonadotropin hCG. The molecular, pharmacological, and morphological characterization of this receptor in MA-10 mouse tumor Leydig cells has been extensively studied (*2, 19, 27, 29*). We report herein that PBR exists mainly as an 18 kDa monomer in control samples. However, within 1 min upon addition of hCG the formation of PBR polymers was detected (Figure 4). Interestingly, the formation of polymers parallels the hCG-induced formation of ROS. The induction of ROS formation in response to gonadotropins has been reported (*41, 42*). This might be due to the initiation of the cytochrome P450 reaction responsible for the metabolism of cholesterol (preexisting in the mitochondria) to pregnenolone and known to generate ROS. The formation of SDS- and mercaptoethanol-resistant (covalent) PBR polymers in response to hCG is also in agreement with our previous studies using transmission electron and atomic force microcopy studies on MA-10 mitochondrial membranes isolated from hormone-treated cells (*29*). The kinetics of the formation of PBR protein polymers, changes in PBR topography (*29*), and PBR ligand binding characteristics are similar and rapid (<1 min). The only apparent discrepancy comes from the data reported herein on MA-10 cells, where PBR mostly
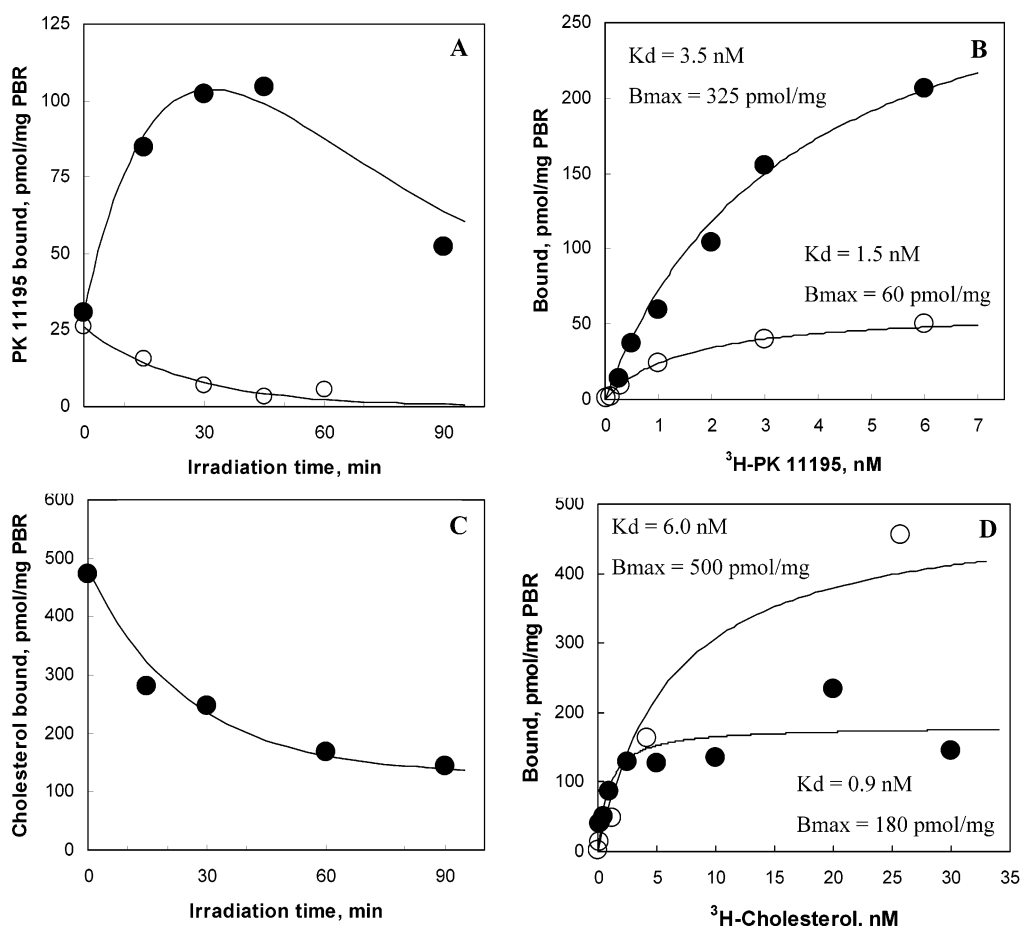
FIGURE 8: Irradiation time dependence and saturation isotherms of [³H]PK 11195 and [³H]cholesterol binding to reconstituted recombinant PBR. Recombinant mouse PBR protein (0.5−2.0 $\mu$g/mL) reconstituted in a 4/1 (w/w) lipid (DMPC/DMPE, 9/1) to protein ratio was used. (A, C) Proteoliposomes were exposed to UV irradiation for the indicated time points. (B, D) 45 min irradiated (closed circles) and nonirradiated (open circles) proteoliposomes were used for binding experiments using either [³H]PK 11195 (B) or [³H]cholesterol (D). Assays were performed and analyzed as described under Experimental Procedures. In (A) the effect of 1 $\mu$M progesterone on PK 11195 ligand binding to irradiated proteoliposomes is shown in open circles. In (B) and (D) the saturation curves, $K_d$, and $B_{max}$ values were obtained by Curve Fit analyses. Results shown are representative of three independent experiments performed in triplicate. The SEM values for $K_d$ and $B_{max}$ were consistently less than 15% of the mean.

exists in its monomeric form in unstimulated cells, and the previous morphological data (28), where in control cells only 40% of PBR was monomeric. This discrepancy could be due to the difference in methodological approaches used in the two studies and the possibility that the polymers seen in control cells by immunogold microscopy were only clustered rather than covalently bound. In contrast, PBR polymers present in Leydig and breast cancer cells seem to involve covalent cross-links resistant to SDS, mercaptoethanol, ethanol, heat, urea, guanidine isothiocyanate, and PBR drug ligands. Moreover, the presence of these complexes was more pronounced when cells or cell lysates were exposed to daylight (data not shown), further indicating the photosensitivity of PBR monomers. These results are in agreement with the data reported by Yeliseev and Kaplan in *Rhodobacter sphaeroides*, a bacterium that contains the tryptophan-rich sensory protein (TspO), a PBR homologue, proposed to serve as an oxygen/light sensor (58).

In addition to the studies performed in cells, in vitro studies were performed to assess the ability of the mouse PBR cDNA to be transcribed and translated to radiolabeled 18 kDa protein and to be incorporated into mitochondria. During these experiments, we observed that, in addition to the major

radiolabeled 18 kDa PBR protein, radiolabeled proteins of 36, 54, and 72 kDa were formed and incorporated into mitochondria. Although in these studies, as well as in the cell studies, we cannot exclude the possibility that these proteins may not be homopolymers but the results of the association of the 18 kDa PBR protein with other proteins (heteropolymers), the observation that these proteins are multiples of 18 kDa makes this possibility less likely. These data were extended in in vitro experiments using His-tagged recombinant PBR protein in solution where PBR dimers were identified by both anti-PBR and anti-His tag antibodies. Furthermore, isolated recPBR protein was shown to form dimers and polymers both in solution and after reconstitution in proteoliposomes in vitro. UV irradiation dramatically increased the formation of these polymers. The fact that recPBR protein alone forms polymers further suggests that the in vivo seen polymers are homopolymers.

Our spectroscopic studies (Figure 5) strongly suggested that tyrosines are involved in the UV irradiation induced cross-link by formation of dityrosines, linking tyrosines belonging to PBR monomers. The presence of PBR trimers and tetramers suggests that there are at least two tyrosines per monomer involved in the polymer formation in a covalent
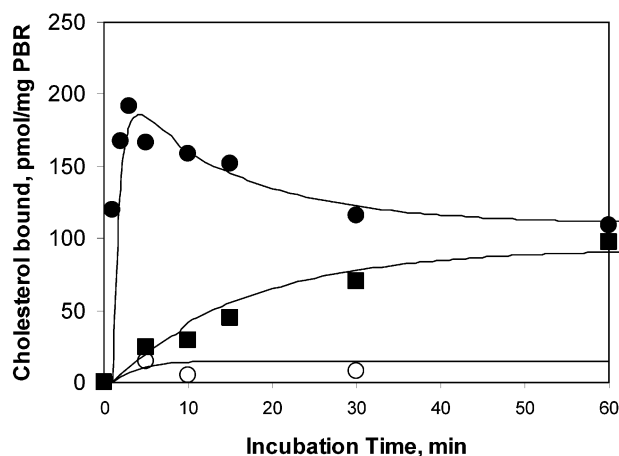
FIGURE 9: Ligand-induced cholesterol binding by PBR polymers in proteoliposomes. Time course of cholesterol binding (6 nM) to either 45 min UV photoirradiated (closed circles) or nonirradiated (closed squares) reconstituted recombinant PBR. Recombinant mouse PBR protein (3.0 $\mu$g/mL) reconstituted in a 4/1 (w/w) lipid (DMPC/DMPE, 9/1) to protein ratio was used. Open circles indicate the effect of 1 $\mu$M progesterone, in the presence of 100 nM PK 11195, on cholesterol binding (6 nM) to irradiated proteoliposomes.

manner. It should be noted that mouse PBR contains 10 tyrosines, some of them located at the amino terminus and others at the carboxy terminus and in the first loop joining the first two transmembrane helices (*59, 60*). On the basis of secondary structure prediction, six of the tyrosines would be in the transmembrane region and probably less accessible for dityrosine formation. From the remaining tyrosines, the reduction in cholesterol binding observed after polymer formation (Figure 8C,D) suggests that Y152 and/or Y153 are probably involved in PBR polymer formation. Indeed, it has been shown that cholesterol binding occurs at the carboxy-terminal domain of PBR and, more specifically, amino acids 150−156 (*2*). The decrease (>60%) in the amount of cholesterol bound to PBR polymers (Figure 8C) correlates with the reduction of PBR monomer levels seen under these experimental conditions in SDS−PAGE (Figure 3), suggesting that only the monomer binds cholesterol or, alternatively, that only one monomer among the polymers binds cholesterol. It cannot be excluded that the decreased ability of the polymers to bind cholesterol could also be due to a conformational change in PBR. In addition, the role of tyrosines in PBR polymer formation was further supported by site-directed mutagenesis experiments where specific tyrosines in PBR were replaced by other amino acids, resulting in a dramatic decrease in polymer formation (unpublished data).

In addition, the proximity of PBR monomers seems rather an important factor for the formation of covalent cross-links, as illustrated by the fact that, in reconstituted proteoliposomes, varying L/P from 4 to 20 (for instance) reduces drastically the formation of trimers and tetramers (compare gels in Figures 3 and 6). However, dimers are always present, suggesting that interactions between two monomers occur naturally under physiological conditions. Image analysis of the freeze-fractured proteoliposomes revealed that 50% of PBR are forming dimers, whereas SDS−PAGE followed by silver staining of the separated proteins showed only 10% of covalently cross-linked PBR multimers. Increased levels of ROS induced trimer and higher molecular mass polymer

formation. This can be regarded in the light of freeze−fracture experiments, which clearly show that dimers are observed even in the absence of any irradiation (Figure 7). Thus, it seems that the efficiency of dityrosine formation is dependent, in addition to L/P ratio, on other parameters to be determined. The "natural" formation of PBR dimers was further supported by PBR expression studies in bacteria where recombinant PBR appeared as 20 and 40 kDa proteins identified with antibodies raised against both PBR and the His tag (Figure 2A).

It is of special interest the finding that a higher rate of polymers is formed when solubilized PBR is photoirradiated in the presence of radiolabeled promegestone and other steroids, including progesterone and pregnenolone but not cholesterol. As noted previously, we used radiolabeled promegestone to study the interaction of cholesterol with the isolated recombinant PBR. Under these conditions, PBR in solution has a lower affinity for promegestone (100 $\mu$M) compared to its affinity for cholesterol (1 $\mu$M) (*2*). These data suggest that cholesterol might prevent covalent PBR cross-linking and thus polymer formation (Figure 2B), whereas other steroids in the presence of UV light favor this process. Thus, the increased formation of PBR polymers in solution compared to reconstituted PBR might be due to a higher diffusion of the PBR monomers in solution. However, the failure of PBR in solution to bind PK 11195 (*2*) suggests that this higher diffusion does not allow for the formation of stable polymers required for PBR ligand binding. Indeed, we previously demonstrated that reincorporation of recPBR into proteolipososomes was required for the receptor to recover the drug ligand binding function (*3*). In the present study we observed that polymer formation increased PK 11195 ligand binding to the receptor (Figure 8A,B) while progesterone abolished the ability of PBR polymers to bind PK 11195 (Figure 8A). To bring this finding into a physiological context, one should consider that, in the steroid biosynthetic pathway, cholesterol is metabolized into pregnenolone, a step occurring into mitochondria, and pregnenolone is then transformed into progesterone by the 3$\beta$-hydroxysteroid dehydrogenase enzyme also found in the mitochondria (*61*). Considering (i) the finding that progesterone does not affect the photoirradiation-induced PBR polymer formation (data not shown), (ii) the data in Figure 2C showing that the UV-photoactivatable derivative of progesterone, promegestone, favors PBR polymer formation in the presence of progesterone, and (iii) the fact that progesterone inhibits drug ligand binding to PBR polymers, it is speculated that progesterone is a critical physiological factor in the regulation of PBR polymerization and function.

We and others have shown that high-affinity PBR drug ligands, such as PK 11195, increase cholesterol transport into mitochondria and the subsequent steroid synthesis by gonadal, adrenal, brain, and liver cells (*62*). We report here that PK 11195 at nanomolar concentrations induced a dramatic increase of cholesterol binding rate by PBR polymers with a half-life of 30 s (Figure 9). Such a rapid process correlates with the in vivo studies on PBR aggregation induced by hCG and its second messenger cAMP in Leydig cells (*29*) and with the well-characterized acute stimulation of steroid synthesis by peptide hormones (*63*). Moreover, as described above for PK 11195 binding,
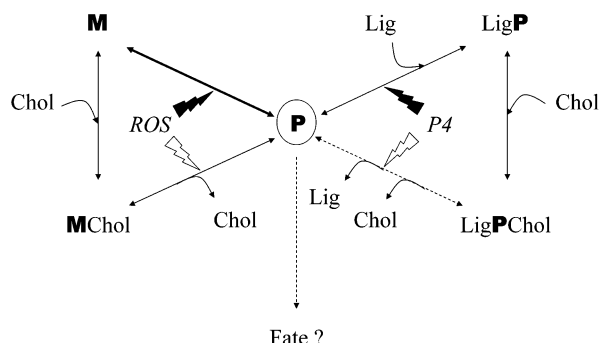
Delavoie et al.



Fate ?

FIGURE 10: Schematic representation of PBR functional states. Additional abbreviations used are PBR monomer (M), polymer (P), cholesterol (Chol), ligands (Lig), reactive oxygen species (ROS), and progesterone (P4).

progesterone, in the presence of PK 11195, was found to inhibit cholesterol binding to PBR polymers (Figure 9).

In aggressive human breast cancer cells, which contain mainly a PBR dimer probably due to the high endogenous free radical levels, PK 11195 increased cholesterol transport into the nucleus and cell proliferation (*32*). This finding is also in agreement with the PK 11195-induced increase of cholesterol binding rate by PBR polymers in vitro.

In an attempt to summarize the function of the monomeric and polymeric forms of the 18 kDa PBR protein, we propose the scheme shown in Figure 10. PBR monomer (M) to polymer (P) transition is driven by ROS. The monomer binds cholesterol (Chol) with high affinity but not PBR ligands (Lig). The presence of cholesterol on the PBR monomer prevents the ROS-induced polymer formation. The polymer binds PBR ligands with high affinity, and ligand binding induces rapid cholesterol binding. This process would allow a membrane that contains PBR to uptake high levels of cholesterol in a time- and ligand-dependent manner. Since progesterone (P4) inhibits both ligand and cholesterol binding to PBR polymer, we suggest that this cholesterol metabolite might be the key element in releasing cholesterol from PBR. Thus, cholesterol could be taken up and released inside a membrane.

A fraction of ligand- and cholesterol-free covalent polymers would be destined to degradation (Fate), thus avoiding the detrimental effects of the presence of high levels of polymers in the mitochondrial membrane. At the same time, newly synthesized monomers will replace PBR in the membrane. Because such a process might take hours, it is possible that only a fraction of the PBR is used at any given time. In such cases, tissues rich in PBR, such as steroid synthesizing tissues, would have continuously available a pool of PBR monomers available for cholesterol transport. It is evident that further studies are required to validate the above proposed model of PBR cycle.

## ACKNOWLEDGMENT

## REFERENCES

1. Braestrup, C., and Squires, R. F. (1977) *Proc. Natl. Acad. Sci. U.S.A. 74*, 3805−3809.
2. Li, H., Yao, Z., Degenhardt, B., Teper, G., and Papadopoulos, V. (2001) *Proc. Natl. Acad. Sci. U.S.A. 98*, 1267−1272.
3. Lacapère, J. J., Delavoie, F., Li, H., Péranzi, G., Maccario, J., Papadopoulos, V., and Vidic, B. (2001) *Biochem. Biophys. Res. Commun. 284*, 536−641.
4. Papadopoulos, V. (1993) *Endocrine Rev. 14*, 222−240.
5. Gavish, M., Bachman, I., Shoukrun, R., Katz, Y., Veenman, L., Weisinger, G., and Weizman, A. (1999) *Pharmacol. Rev. 51*, 629−650.
6. Casellas, P., Galiegue, S., and Basile, A. S. (2002) *Neurochem. Int. 40*, 475−486.
7. Benavides, J., Manager, J., Burgevin, M. C., Ferris, O., Uzan, A., Gueremy, C., Renault, C., and Le Fur, G. (1985) *Biochem. Pharmacol. 34*, 167−170.
8. Gavish, M., and Fares, F. (1985) *J. Neurosci. 5*, 2889−2893.
9. Awad, M., and Gavish, M. (1989) *J. Neurochem. 52*, 1880−1885.
10. Schoemaker, H., Boles, R. G., Horst, W. D., and Yamamura, H. I. (1983) *J. Pharmacol. Exp. Ther. 225*, 61−69.
11. Le Fur, G., Perrier, M. L., Vaucher, N., Imbault, F., Flamier, A., Uzan, A., Renault, C., Dubroeucq, M. C., and Gueremy, C. (1983) *Life Sci. 32*, 1839−1847.
12. Doble, A., Ferris, O., Burgevin, M. C., Menager, J., Uzan, A., Dubroeucq, M. C., Renault, C., Gueremy, C., and Le Fur, G. (1987) *Mol. Pharmacol. 31*, 42−49.
13. Antkiewicz-Michaluk, L., Guidotti, A., and Krueger, K. E. (1988) *Mol. Pharmacol. 34*, 272−278.
14. Riond, J., Vita, N., Le Fur, G., and Ferrara, P. (1989) *FEBS Lett. 245*, 238−244.
15. Parola, A. L., Putnam, C. W., Russell, D. H., and Laird, H. E., II (1989) *J. Pharmacol. Exp. Ther. 250*, 1149−1155.
16. Sprengel, R., Werner, P., Seeburg, P. H., Mukhin, A. G., Santi, M. R., Grayson, D. R., Guidotti, A., and Krueger, K. E. (1989) *J. Biol. Chem. 264*, 20415−20421.
17. Riond, J., Mattei, M. G., Kaghad, M., Dumont, X., Guillemot, J. C., Le Fur, G., Caput, D., and Ferrara, P. (1991) *Eur. J. Biochem. 195*, 305−311.
18. Parola, A. L., Stump, D. G., Pepperl, D. J., Krueger, K. E., Regan, J. W., Laird, H. E., II (1991) *J. Biol. Chem. 266*, 14082−14087.
19. Garnier, M., Dimchev, A. B., Boujrad, N., Price, J. M., Musto, N. A., and Papadopoulos, V. (1994) *Mol. Pharmacol. 45*, 201−211.
20. Doble, A., Benavides, J., Ferris, O., Bertrand, P., Menager, J., Vaucher, N., Burgevin, M. C., Uzan, A., Gueremy, C., and Le Fur, G. (1985) *Eur. J. Pharmacol. 119*, 153−167.
21. Snyder, S. H., Verma, A., and Trifiletti, R. R. (1987) *FASEB J. 1*, 282−288.
22. Lueddens, H. W. M., Newman, A. H., Rice, K. C., and Skolnick, P. (1986) *Mol. Pharmacol. 29*, 540−545.
23. McCabe, R. T., Schoenheimer, J. A., Skolnick, P., Hauck-Newman, A., Rice, K., Reig, J.-A., and Klein, D. C. (1989) *FEBS Lett. 244*, 263−267.
24. Paul, S. M., Kempner, E. S., and Skolnick, P. (1981) *Eur. J. Pharmacol. 76*, 465−466.
25. McEnery, M. W., Snowman, A. M., Trifiletti, R. R., and Snyder, S. H. (1992) *Proc. Natl. Acad. Sci. U.S.A. 89*, 3170−3174.
26. Golani, I., Weizman, A., Leschiner, S., Spanier, I., Eckstein, N., Limor, R., Yanai, J., Maaser, K., Scherubl, H., Weisinger, G., and Gavish, M. (2001) *Biochemistry 40*, 10213−10222.
27. Papadopoulos, V., Mukhin, A. G., Costa, E., and Krueger, K. E. (1990) *J. Biol. Chem. 265*, 3772−3779.
28. Papadopoulos, V., Boujrad, N., Ikonomovic, M., Ferrara, P., and Vidic, B. (1994) *Mol. Cell. Endocrinol. 104*, R5−R9.
29. Boujrad, N., Vidic, B., and Papadopoulos, V. (1996) *Endocrinology 137*, 5727−5730.
30. Joseph-Liauzun, E., Farges, R., Delmas, P., Ferrara, P., and Loison, G. (1997) *J. Biol. Chem. 272*, 28102−28106.
31. Veenman, L., Leschiner, S., Spanier, I., Weisinger, G., Weizman, A., and Gavish, M. (2002) *J. Neurochem. 80*, 917−927.
32. Hardwick, M., Fertikh, D., Culty, M., Li, H., Vidic, B., and Papadopoulos, V. (1999) *Cancer Res. 59*, 831−842.

33. Yao, Z., Drieu, K., and Papadopoulos, V. (2001) *Brain Res. 889*, 181−190.
34. Bradford, M. M. (1976) *Anal. Biochem. 72*, 248−254.
35. Whalin, M., Boujrad, N., Papadopoulos, V., and Krueger, K. E. (1994) *J. Recept. Res. 14*, 217−228.
36. Amri, H., Ogwuegbu, S. O., Boujrad, N., Drieu, K., and Papadopoulos, V. (1996) *Endocrinology 137*, 5707−5718.
37. Li, H., and Papadopoulos, V. (1998) *Endocrinology 139*, 4991−4997.
38. Morrissey, J. H. (1981) *Anal. Biochem. 117*, 307−310.
39. Malencik, D. A., Sprouse, J. F., Swanson, C. A., and Anderson, S. R. (1996) *Anal. Biochem. 242*, 202−213.
40. Davies, M. J., Fu, S., Wang, H., and Dean, R. T. (1999) *Free Radical Biol. Med. 27*, 1151−1163.
41. Peltola, V., Huhtaniemi, I., Metsa-Ketela, T., and Ahotupa, M. (1996) *Endocrinology 137*, 105−112.
42. Sawada, M., and Carlson, J. V. (1996) *Endocrinology 137*, 1580−1584.
43. Maskos, Z., Rush, J. D., and Koppenol, W. H. (1992) *Arch. Biochem. Biophys. 296*, 514−520.
44. Van der Vlies, D., Pap, E. H., Post, J. A., Celis, J. E., and Wirtz, K. W. (2002) *Biochem. J. 366*, 825−830.
45. Kanwar, R., and Balasubramanian, D. (2000) *Biochemistry 39*, 14976−14983.
46. Peranzi, G., Bayle, D., Telford, J. N., and Soumarmon, A. (1994) *Biol. Cell 73*, 163−171.
47. Maccario, J., Peranzi, G., Bayle, D., Lewin, M. J., and Thomas-Soumarmon, A. (1994) *Biol. Cell 80*, 55−62.
48. Hirsch, J. D., Beyer, C. F., Malkowitz, L., Beer, B., and Blume, A. J. (1988) *Mol. Pharmacol. 34*, 157−163.
49. Ikezaki, K., and Black, K. L. (1990) *Cancer Lett. 49*, 115−120.
50. Miettinen, H., Kononen, J., Haapasalo, H., Helén, P., Sallinen, P., Harjuntausta, T., Helin, H., and Alho, H. (1995) *Cancer Res. 55*, 2691−2695.
51. Papadopoulos, V., Dharmarajan, A. M., Li, H., Culty, M., Lemay, M., and Sridaran, R. (1999) *Biochem. Pharmacol. 58*, 1389−1393.
52. Maaser, K., Hoper, M., Jansen, A., Weisinger, G., Gavish, M., Kozikowski, A. P., Weizman, A., Carayon, P., Riecken, E. O., Zeitz, M., and Scherubl, H. (2001) *Br. J. Cancer 85*, 1771−1780.
53. Decaudin, D., Castedo, M., Nemati, F., Beurdeley-Thomas, A., DePinieux, G., Caron, A., Pouillard, P., Wijdenes, J., Rouillard, D., Kroemer, G., and Poupon, M. F. (2002) *Cancer Res. 62*, 1388−1393.
54. Strohmeier, R., Roller, M., Sanger, N., Knecht, R., and Kuhl, H. (2002) *Biochem. Pharmacol. 64*, 99−107.
55. Brown, R. C., and Papadopoulos, V. (2001) *Int. Rev. Neurobiol. 46*, 117−144.
56. Szatrowski, T. P., and Nathan, C. F. (1991) *Cancer Res. 51*, 794−798.
57. Brown, N. S., and Bicknell, R. (2001) *Breast Cancer Res. 3*, 323−327.
58. Yeliseev, A. A., and Kaplan, S. A. (1995) *J. Biol. Chem. 270*, 21167−21175.
59. Joseph-Liauzun, E., Delmas, P., Shire, D., and Ferrara, P. (1998) *J. Biol. Chem. 273*, 2146−2152.
60. Culty, M., Li, H., Boujrad, N., Amri, H., Vidic, B., Bernassau, J. M., Reversat, J. L., and Papadopoulos, V. (1999) *Steroid Biochem. Mol. Biol. 69*, 123−130.
61. Cherradi, N., Defaye, G., and Chambaz, E. M. (1994) *Endocrinology 134*, 1358−1364.
62. Papadopoulos, V. (1998) *Proc. Soc. Exp. Biol. Med. 217*, 130−142.
63. Jefcoate, C. R., McNamara, B. C., Artemenko, I., and Yamazaki, T. (1992) *J. Steroid Biochem. Mol. Biol. 43*, 751−767.